Available online at www.sciencedirect.com

ScienceDirect

00 (2016) 1–15

Journal Logo

A neural model of the frontal eye fields with reward-based learning

Weijie Ye[a], Shenquan Liu[a,*], Xuanliang Liu[a], Yuguo Yu[b]

[a]*School of Mathematics, South China University of Technology, Guangzhou, 510640, China*
[b]*Center for Computational Systems Biology, The State Key Laboratory of Medical Neurobiology and Institutes of Brain Science, Fudan University, School of Life Sciences, Shanghai, 200433, China*

Abstract

Decision-making is a flexible process dependent on the accumulation of various kinds of information; however, the corresponding neural mechanisms are far from clear. We extended a layered model of the frontal eye field to a learning-based model, using computational simulations to explain the cognitive process of choice tasks. The core of this extended model has three aspects: direction-preferred populations that cluster together the neurons with the same orientation preference, rule modules that control different rule-dependent activities, and reward-based synaptic plasticity that modulates connections to flexibly change the decision according to task demands. After repeated attempts in a number of trials, the network successfully simulated three decision choice tasks: an anti-saccade task, a no-go task, and an associative task. We found that synaptic plasticity can modulate the competition of choices by suppressing erroneous choices while enhancing the correct (rewarding) choice. In addition, the trained model captured some properties exhibited in animal and human experiments, such as the latency of the reaction time distribution of anti-saccades, the stop signal mechanism for canceling a reflexive saccade, and the variation of latency to half-max selectivity. Furthermore, the trained model was capable of reproducing the re-learning procedures when switching tasks and reversing the cue-saccade association.

Keywords: Decision-making, Task switching, Reward-based Hebbian learning, Direction-preferred population

1. Introduction

Decision-making in the presence of multiple choices requires more than sensory signaling and motor response. Information accumulation and processing are also necessary for decision-making (Salinas, 2004; Savine and Braver, 2010; Noorani, 2014). Decision-making is a flexible process of integrating various forms of information, such as past experience and learning rules (Drugowitsch et al., 2012; Cutsuridis et al., 2014; Pleger et al., 2006; Chaumon et al., 2014; Kan et al., 2012). In an anti-saccade testing paradigm, which is an important tool for estimating frontal lobe dysfunction, trial-by-trial training can alter the visuomotor mapping of macaques and make them saccade to the opposite side against the reflexive response (Munoz and Everling, 2004). Based on this kind of flexibility, humans and other animals are capable of responding to a specific stimulus in different ways (Drea and Wallen, 1999; Platt and Glimcher, 1999).

The visuomotor choice tasks, such as the anti-saccade task and no-go task, have been widely used to investigate the cognitive process of decision-making, because a saccadic eye movement can readily represent the behavioral outcome (SchlagRey et al., 1997; Hutton, 2008; Leathers and Olson, 2012). These experiments study the process of accumulating experience and integrating information. The goal of these tasks is to perform planned eye movements in response to learned stimuli, and the decision is signaled to be correct by reward. At the end of a trial, rewards can be given based on the performance of this sensory-triggered activity, instructing animals to learn the "correct" visuomotor mappings and suppress the "erroneous" choices (Munoz and Everling, 2004; Baldassarre et al., 2013; Blank et al., 2013). In other words, the brain will re-establish the link between the ongoing sensory signals and behavioral results, under the guidance of rewards (Brown et al., 2004; Luhmann et al., 2008). Some experimental findings have emphasized the role of synaptic plasticity in the functional neural circuits in the frontal eye fields (FEF), which play a key role in oculomotor control of saccadic eye movements and visual attention. For example, Chen and Wise (1995b) observed learning-dependent and learning-selective activities in FEF. Bichot et al. (1996) discovered a type of experience-dependent plasticity that mediated the learning of arbitrary stimulus-action associations. Recent results present more evidence that learning in oculomotor behaviors involves FEF (Lee and Keller, 2008; Tseng et al., 2013; Lewis et al., 2009). All these findings provide support for synaptic plasticity in FEF.

*Corresponding author. E-mail address: mashqliu@scut.edu.cn

In this study, we extended the layered FEF model introduced by Heinzle et al. (2007) into a learning-based model, shedding more light on the cognitive process of choice tasks. The modification of the model includes four aspects: (1) The recognition module and layer 6 were removed and the model could initially only cause a reflexive saccade (pro-saccade). (2) Two rule modules were added to the fixation input layer. These modules not only reserved the function of fixation neurons, but could also transform the color signal from V4 into rule-based control. Meanwhile, two functional units were divided out of layer 2/3 to represent the rule-dependent neurons that are controlled by the rule modules. Interestingly, the rule-preferred activity has been observed in FEF and other parts of the frontal cortex (Hoshi et al., 1998; White and Wise, 1999; Ferrera et al., 1999; Asaad et al., 2000; Everling and Munoz, 2000; Hasegawa et al., 2004; Everling and DeSouza, 2005; Johnston and Everling, 2006; Johnston et al., 2007). In the work of Johnston et al. (2009), a mechanism based on two functional populations has been proposed to account for task selectivity in the prefrontal cortex. All these evidence support the rule module in our model. (3) The populations had direction preference, i.e. different populations in a layer preferred specific directions. Orientation selectivity in FEF has been extensively researched (Douglas et al., 1991; Li and Creutzfeldt, 1984; Schiller et al., 1976; Ringach et al., 2002; Nowak et al., 2008; Hansel and van Vreeswijk, 2012; Hubel and Wiesel, 1959). Additionally, an increasing number of models have applied this property to distinct functional modules to simulate various physiological experiments (Engel and Wang, 2011; Ardid and Wang, 2013; Shushruth et al., 2012; Wu and Guo, 2011; Zirnsak et al., 2011). (4) We assumed that the connections from layer 4 to layer 2/3 were plastic, employing reward-based Hebbian learning (Pfeiffer et al., 2010; Engel and Wang, 2011; Ardid and Wang, 2013). In the present model, the connection between E4 and I23 which did not exist in the original model was considered to be weakly linked and plastic. These plastic synapses simulated the varying inputs to the neuronal population that was involved in the accumulation of sensory information, allowing decision-making to be guided by the associated values of the choices (Gottlieb et al., 2014; Gold and Shadlen, 2002, 2003; Law and Gold, 2009; Connolly et al., 2009).

In order to gain insight into the effect of the plasticity on controlling the oculomotor behaviors in FEF, we trained the extended model to simulate three different choice tasks: an anti-saccade task, a no-go task, and an associative task. The simulation results successfully accounted for the learning processes, and quantitatively exhibited the cognitive procedure of decision-making. They also could explain the relearning processes when tasks switched without an explicit cue. The extended model generalizes the learning mechanism to the saccade control in FEF so that it can choose or switch between multiple sensory-motor maps, suggesting that the plasticity plays an important role in flexibly controlling the saccade movements.

2. Method

2.1. Network architecture

The architecture of the learning-based FEF model is illustrated in Fig. 1A. This extended model consists of interacting layers contributing to different functions: sensory processing in layer 4 (L4), attention allocating in layer 2/3 (L23), fixation input layer (FIX) and motor output in layer 5 (L5). L4 neurons process orientation-preferred visual input from early visual areas. L23 serves as an attention allocator as it transforms the sensory signal from L4 into the attention signal at a direction-preferred position. The activities of L23 neurons are similar to those of visuomotor neurons in FEF classified by Bruce and Goldberg (1985). Visuomotor neurons discharge both in response to visual signals and after the visual targets disappear. The response of visuomotor neurons can persist until the monkey makes a saccadic eye movement. Based on the winner-take-all competition and strong recurrent excitation, L23 neurons are able to reproduce these activities of visuomotor neurons. Strong synaptic weights from the excitatory pool in L5B to the inhibitory pool in L23 are required to suppress the L23 neurons when a saccade is made in the present model. L23 is divided into two task-relevant units L23L and L23R which are controlled by the rule neurons in FIX. In addition, we use two populations to simulate the rule neurons which transform the green and red color information from V4 into a rule signal in FIX (Fig. 1C). The third population in FIX only processes fixation input without color information. For the sake of simplicity, we have designed the network so that E23L and E23R are inhibited by the red and green rule neurons through connecting FIX to I23L and I23R, respectively. L5 is comprised of two types of neurons: ramping motor neurons (L5R) and burst motor neurons (L5B), which integrate attention signals and signal the motor output, respectively. The ramping activities of L5R are inhibited by FIX. Except FIX, each layer has 13 retinotopic positions which have their own preferred direction (Fig. 1B). It is noteworthy that a retinotopic position consists of a different number of neurons in different layers. In L4 and L23, each position contains 100 excitatory neurons and 25 inhibitory neurons, while L5 is composed of 40 excitatory and 25 inhibitory neurons. FIX has 100 neurons in each of the three excitatory populations, and 75 inhibitory neurons.

2.2. Neuronal dynamics

Each neuron is modeled as an integrate-and-fire model which is described by

$$\tau_m \frac{dV}{dt} = -V - g_{exc}(V - V_e) - g_{inh}(V - V_i) + I_{ext} \qquad (1)$$

where V represents the membrane potential, τ_m is the membrane time constant, $\tau_m = 20$ ms in excitatory neurons and $\tau_m = 12$ ms in inhibitory neurons, and $V_e = 74$ mV, $V_i = -10$ mV denote the excitatory and inhibitory reversal potentials. The conductance g_{exc} and g_{inh} consist of three distinct parts $g_{e,i}$, g_{noise} and $g_{plastic}$ which represent synaptic conductance, noise input and the plastic synapse. The spiking threshold is 20 mV,

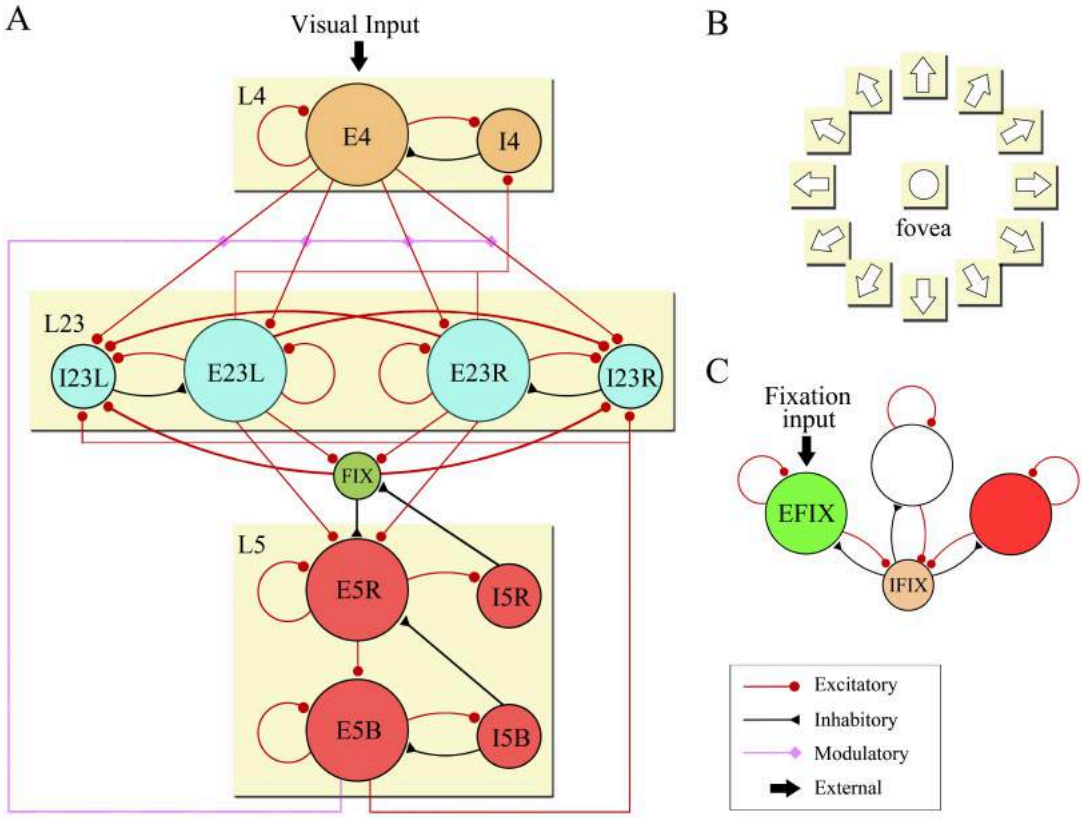

Figure 1. Network architecture of the learning-based model. (A) The network structure has four layers that simulate different cognitive processes: sensory processing (L4), attention allocation (L23), fixation input (FIX), and motor output (L5R and L5B). Each layer has an excitatory pool and an inhibitory pool. (B) A functional pool consists of 13 retinotopic positions. Except the fovea position, each retinotopic position prefers a distinct orientation. Each retinotopic position denotes a population of neurons. (C) FIX has three excitatory populations (EFIX) and one inhibitory population (IFIX). Two of the excitatory populations encode the green and red color fixation input while the other only processes fixation input without color information.

and reset value is 10 mV. The absolute refractory period of excitatory and inhibitory neurons are 1.8 ms and 1.2 ms, respectively. First, the synaptic conductance is given by

$$\begin{aligned} g_{e,i}^{k\to j} &= \sum_{l} g_{kj} s_{e,i}^{k\to j} \\ \tau_{e,i}\frac{ds_{e,i}}{dt} &= -s_{e,i} \end{aligned} \tag{2}$$

where $s_{e,i}$ is the activation variable and $\tau_{e,i}$ is the time constant of excitatory and inhibitory synapses. Different connections are given different time constants: $\tau_{e,i}$ = 50 ms in the connection E5R→E5R, $\tau_{e,i}$ = 10 ms in the connections E23L→E23L, E23R→E23R, I5B→E5R, and $\tau_{e,i}$ = 5 ms in the other connections. g_{kj} denotes the direction preference factor between neurons with preferred directions θ_k and θ_j (Ardid et al., 2007). This factor is determined by a Gaussian function:

$$g_{kj}(\theta_k - \theta_j) = g_a e^{\left(-\frac{(\theta_k-\theta_j)^2}{2\sigma^2}\right)} \tag{3}$$

where $\sigma = 18°$, g_a = 1.0. As an exception, g_a between E4 and I23 is 0.01, denoting the weak link. It is noted that the fovea is considered to be next to other retinotopic positions, and g_{kj} between them is $g_{kj}(30°)$.

Second, the noise input mimics the noisy background inputs within the brain (Destexhe et al., 2001; Salinas, 2003; Moreno-Bote and Parga, 2004, 2010) and obeys:

$$\tau_{noise}\frac{dg_{noise}}{dt} = -(g_{noise} - \mu) + \sqrt{\frac{\mu w_{e,i}}{\tau_{noise}}}\chi(t) \tag{4}$$

where $\chi(t)$ is a random variable that follows a Gaussian distribution with mean 0 and standard deviation of 1. μ is the mean external input. The time constant τ_{noise} = 3 ms and the external weights are w_e = 0.02 and w_i = 0.06.

Third, the synapses from L4 to L23 are plastic. The plastic connection can be either depressing or potentiating. For simplicity, the plastic synapses project to the connections from E4 to E23L (E23R) and from E4 to I23L (I23R) refer to left (right) excitatory modulation and left (right) inhibitory modulation, respectively. They are described by (Pfeiffer et al., 2010; Engel and Wang, 2011; Ardid and Wang, 2013):

$$g_{plastic}^{k} = g_p \sum_{j} c_{kj} \tag{5}$$

where g_p = 1.0 , c_{kj} gives the strength of the plastic input. At the end of a training trial, the presynaptic and postsynaptic

activities determine all plastic synapses to be depressed or potentiated. Then, synapses will update according to a Hebbian reward-dependent learning rule. In this process, the transition to potentiation state is given by $c \rightarrow c + q \cdot Q(S_{max})(1 - c)$, while depression is governed by $c \rightarrow c - q \cdot Q(S_{max})c$. Learning rate with $q = 0.03$ in excitatory-based plastic synapses and $q = 0.01$ in inhibitory-based plastic synapses. The plasticity rate $Q(S_{max})$ gradually depends on the maximum presynaptic firing rate S_{max}:

$$Q(S_{max}) = \left(1 + e^{\frac{(S_0 - S_{max})}{\tau_q}}\right)^{-1} \tag{6}$$

where $S_{max} = \max(S(t))$ denotes the maximum population firing rate of the presynaptic population, and the population firing rate $S(t)$ is described below. $S_0 = 60$ Hz and $\tau_q = 5$ Hz, which give the activity threshold and slope constant, respectively. The stimulus to L4 is also set to be direction-preferred which obeys:

$$I_{ext}(\theta) = I_M e^{\left(-\frac{(\theta-\theta_p)^2}{2(\sigma_s)^2}\right)} \tag{7}$$

where $I_M = 0.056$ nA, $\sigma_s = 15^\circ$ and θ_p represents the preferred orientation. The fixation input is 0.8 nA.

2.3. Task simulation and analysis

Using Hebbian reward-dependent learning, we simulated the cognitive processes of three choice tasks: no-go task, anti-saccade task and associative task. First, in the no-go task, a fixation cue is presented for 100 ms and then a visual target is shown. This visual target randomly appears in different positions in different trials. At 300 ms, the fixation input without color information, which serves as the stop signal, appears. The network needs to suppress the erroneous saccade and keep "fixating" in the fovea position for 700 ms. If a saccade movement produces between 300 ms and 1000 ms, the trial is counted as failed (erroneous no-go trial). A total of 150 trials are performed for each direction in this task. Second, in the anti-saccade task, a visual target appears after "fixating" on the fovea for 100 ms. This target remains until a saccade occurs. A correct trial requires making a saccade to the opposite side of the visual target. In this task, we train the model in 120 consecutive trials. Note that 20 pre-training trials were processed before the formal training by presenting another stimulus 600 ms after and at the mirror location of the visual target, providing post-trial information about the correct location for the anti-saccade (Everling et al., 1999). In addition, we also simulate task switching with the model. The network performs alternating blocks of pro-saccade tasks and anti-saccade tasks. In one block, only one decision is correct. Without color fixation input, the model has to generate a pro-saccade or an anti-saccade, instructed only by reward. After 30 correct trials, the task switches without any explicit instruction. In this test, 60 blocks are performed. Third, the associative task asks the network to associate the cue stimulus, either left or right, based on the color of fixation input. The paradigm of the task is similar to that used in the works of Asaad et al. (1998) and Pasupathy and Miller (2005). The fixation spot is first shown and lasts for 1600 ms. During this period, a cue stimulus in a direction appears at 100 ms. This cue lasts for 500 ms. After a delay period of 1000 ms, two target stimuli are given on the left side (180°) and the right side (0°). We divide the direction into two categories: (60°, 90°, 120°, 150°, 180°, 210°) for category 1 and (0°, 30°, 240°, 270°, 300°, 330°) for category 2 (Freedman and Assad, 2006). When the green fixation cue is presented, the cue stimulus from category 1 or category 2 is linked to a leftward response or rightward response, respectively. When the red fixation is displayed, these pairings are reversed. A total of 120 trials for each cue stimulus and each fixation input are performed in this task. The total number of trials is 2400. Moreover, task switching is also performed in the trained model, similar to the task switching in anti-saccade task. In this case, the cue stimulus is paired to either the left side or the right side. Once the task switches after 30 correct trials, the cue-saccade pairing reversal occurs without an explicit instruction.

The performance of the tasks is estimated by firing rate in two forms: population firing rate and neural firing rate. Population firing rate is calculated by counting the number of spikes within a population in 1 ms time bins and smoothed by $S(t)$:

$$S(t) = \frac{\left(1 - e^{(-\frac{t}{\tau_{rise}})}\right)e^{(-\frac{t}{\tau_{decay}})}}{\int_0^\infty \left(1 - e^{(-\frac{t'}{\tau_{rise}})}\right)e^{(-\frac{t'}{\tau_{decay}})}dt'} \tag{8}$$

where $\tau_{rise} = 1ms$, $\tau_{decay} = 10ms$. The neural firing rate is determined by the membrane potential of a single neuron:

$$r(V) = \left(1 + e^{\frac{(\gamma - V)}{\beta}}\right)^{-1} \tag{9}$$

where $\beta = 2.0$, $\gamma = 16.5$, which denote the slope constant and threshold, respectively.

In addition, based on the different characteristics of three tasks, three corresponding modulation rate are designed to reveal the average modulation effect of two plastic synapses M^e and M^i:

$$M^{e,i} = \begin{cases} \dfrac{\left\langle \sum_k (g^{e,i}_{plastic(kj)} + g^{e,i}_{syn(kj)}) \right\rangle}{\left\langle \sum_k \sum_j (g^{e,i}_{plastic(kj)} + g^{e,i}_{syn(kj)}) \right\rangle} \\ \dfrac{\left\langle \sum_k (g^{e,i}_{plastic(kj)} + g^{e,i}_{syn(kj)}) \right\rangle}{\left\langle \sum_k (g^{e}_{plastic(kj)} + g^{e}_{syn(kj)}) \right\rangle + \left\langle \sum_k (g^{i}_{plastic(kj)} + g^{i}_{syn(kj)}) \right\rangle} \\ \left\langle \dfrac{g^{e,i}_{plastic(kj)} + g^{e,i}_{syn(kj)}}{\sum_k (g^{e,i}_{plastic(k)} + g^{e,i}_{syn(k)})} \right\rangle \end{cases} \tag{10}$$

The equations, from top to bottom, are applied in the anti-saccade task, no-go task, and associative task, respectively. k and j represent the beginning retinotopic positions and the target retinotopic positions of a synapse, respectively. The calculation $\langle a \rangle$ denotes the trial average of a for each task, repeated 5 times. The modulation ratio is designed to estimate the change of synapse weight and avoid the situation that some synapse weights are close to zero. The modulation ratio of the anti-saccade task denotes the ratio of the sum of all the synapse

weights targeted to the neuron *k* to the sum of all synapse weights. The modulation ratio of the no-go task is the proportion of the sum of the synapse weights targeted to the neuron *k* to the sum of all excitatory- and inhibitory-based synapse weights. For the associative task, it is the ratios of synaptic weight to the sum of synaptic weights targeted to the *k* neuron.

Using Euler method with time steps of 0.1 ms, the simulations were run in MATLAB (MathWorks, Natick, MA). The results did not change significantly when testing with a shorter time step of 0.01 ms.

3. Results

3.1. Pro-saccade with no orientation preference

Before training in tasks, the network was tuned to a state that had two properties: (1) makes a reflexive saccade to the visual target, and (2) has no preference for any visual signal. All choice tasks in this study were based on this initial state. Fig. 2 showed two examples of this state. In the first instance, the network first "fixated" on the fovea at 400 ms, and then target 1 was shown in the 90° direction (Fig. 2A). Once it has made a saccade decision, target 1 input was turned off and the fixation signal displayed 100 ms. The next target then revealed in the 270° direction. After a similar decision process of the first target, a 150° preferred input was applied to the network, and the network would saccade to the corresponding visual target. In E4, persistent activity was triggered by direction-preferred sensory stimuli, processing the spatial visual signals. These persistent visual signals induced a gradual increase in the firing rate of corresponding retinotopic positions. Once the firing rate of a population in E5B reached a threshold, the network would determine to saccade to the corresponding visual target. At the same time, this population inhibited the activities of other retinotopic positions for a short time, depressing the other saccade choices. As a result, these three direction-preferred inputs all gave rise to the corresponding reflexive saccade.

The choice tasks also required that the network did not prefer saccading to one specific target when multiple direction-preferred stimuli were presented simultaneously. The second example illustrates the response of the network as the visual target appears in 0°, 90°, 180° and 270° directions at the same time (Fig. 2B). It could be observed that the decision of saccade was likely to locate at an arbitrary visual target in these four directions. None of these choices was attractive enough to maintain the attention of the network. It should be noted that the non-stimulation population activities were more suppressed when multiple targets were presented, as compared to only one target presented. This was due to L4 in the original model being endowed with winner-take-all competition, making it unable to deal with multiple sensory signals from different directions. This issue was resolved in the present model by weakening the winner-take-all competition in L4 so that the single sensory processing in the present model was analogous to the original model, while allowing sequential winner-changing dynamics behavior with multiple sensory signals.

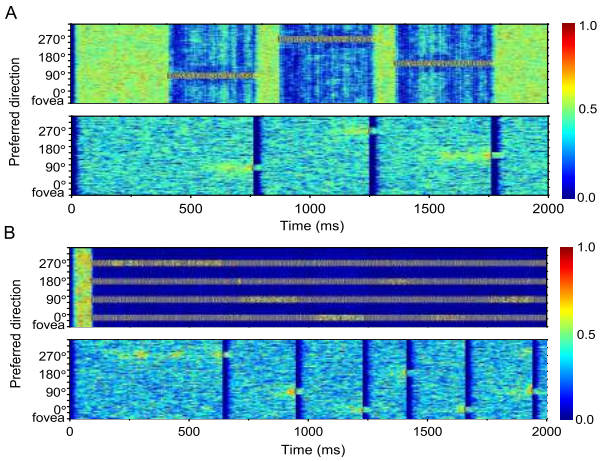

Figure 2. Two examples of the network dynamics over time and retinotopic positions in a pro-saccade task before learning. Colors represent the neuronal firing rate. (A) A pro-saccade test proves that the network can make a reflexive saccade. (B) A test proves that network with no preference for specific direction.

3.2. Anti-saccade task

In the anti-saccade task, the network was trained to saccade to the opposite side of the given cue stimulus. We chose the 90° retinotopic position and its opposite side 270° position as an example of the task. Fig. 3 illustrates the anti-saccade-relevant activities when the network was training. Two graphs plotted variations of the population firing rate in 90° and 270° retinotopic populations, respectively (Fig. 3B). In early trials, the 90° preferred population exhibited overwhelming activity, indicating that the network mainly produced a saccadic movement to the target at 90°. Subsequently, as the network "learned", the firing rate of the 90° retinotopic population declined to a relatively low level. In contrast, the 270° preferred population showed much stronger responses at the end of training. To better capture the characteristics of the process of information accumulation, we computed the saccade percent probability (SPP) of pro-saccade and anti-saccade in a sliding bin with a width of 30 trials, which moved forward by one step in each trial. SPP was defined as the ratio of the number of correct trials to the total number of trials in a bin. The results in Fig. 3B provide an intuitive illustration of the competition between pro-saccade and anti-saccade. Because the pre-training suppressed the activity of pro-saccade, the SPP of pro-saccade in the early bins was around 80% rather than 100%. Although the pro-saccade was the primary decision before approximately the 45th bin, the pro-saccade SPP progressively decreased. In contrast, the number of anti-saccade was enhanced after learning over successive trials. After the 45th bin, the anti-saccade decision dominated and its SPP increased more rapidly. At the end of the task, the network made the anti-saccade decision in more than 90% trials of a bin, indicating it has "learned" the anti-saccade performance. In this process, a natural question arose: How do plastic synapses modulate the network to perform a specific behavior? To quantitatively answer this question, the modulation ratio was designed and calculated (Fig. 3C). It could be observed that the

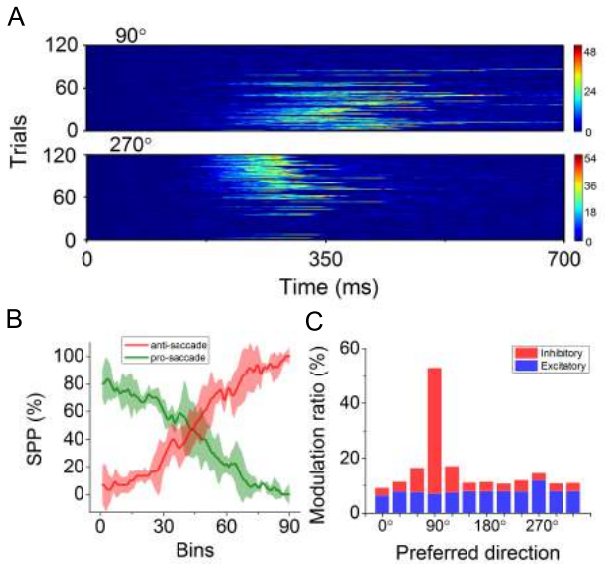

Figure 3. Training process of anti-saccade task. (A) The response of E5R in 90° (top panel) and 270° (bottom panel) preferred population. Colors refer to the population firing rate of E5R. (B) The saccade percent probability of pro-saccade and anti-saccade as a function of bins in training. (C) The modulation ratios of different direction-preferred populations projected by two plastic synapses after training. Here, these two plastic synapses are between L4 and L23R, which are relevant to anti-saccade.

erroneous targets such as 60°, 90° and 120° exhibited a relatively higher inhibitory modulation ratio than the correct choice. By contrast, the excitatory modulation ratios did not produce such a dramatic change. The excitatory modulation ratio of the correct target (270°) was 3.94% higher than the other choices on average. The mechanisms of suppressing erroneous choices and enhancing correct choices by synaptic plasticity accounted for the change in choice behavior.

Fig. 4A illustrates the firing rate time course of the 90° and 270° preferred populations in the trained network. The red fixation input induced tonic activity in FIX. After stimulus onset, the fixation response gradually ramped down, while E4 responded to the visual target. Then E23R was activated by the ongoing sensory signal, indicating that the anti-saccade related attention began to allocate. At the beginning, activity of the 90° preferred population and 270° preferred population increased simultaneously [Fig. 3 in Everling and Munoz (2000);]. Subsequently, the 270° preferred population won the competition so that the network allocated attention to the visual target in this direction. Once the ramping activity of E5R, which was induced by the attention signal, reached a threshold, neurons in E5B rapidly released a motor signal, driving the network to make a saccadic movement to the 270° target [Fig. 2 in Schall et al. (2000); Fig. 5 in Hanes et al. (1998), Fig. 4 in Everling et al. (1999)].

To see whether the trained model can reproduce the latency of anti-saccades in psychophysical experiments, the same pro-saccade task and anti-saccade task were simulated 2000 times, respectively. In total, 93.4%±0.78% accuracy was found in the anti-saccade task, while accuracy was 99.55%±0.92% in the pro-saccade task. Fig. 4B illustrates the reaction time (RT) distribution of these simulations, with RT defined by the time difference between target onset and saccadic movement. It was observed that the RTs of anti-saccade task had higher latency compared to the pro-saccade task. The average RTs in pro-saccade and anti-saccade tasks were 210.15±2.16 ms and 266.01±3.33 ms, respectively. Thus, the average latency of the anti-saccade was evaluated as about 55.86 ms. Similar RT distributions were found in primate experiments (Everling et al., 1998, 1999; Bell et al., 2000; Sander et al., 2010). According to their published data, the time delay of anti-saccades had a range of 13 ms to 77 ms, which is compatible with our results. We also analyzed the distribution of RTs for erroneous responses. The RT distribution of erroneous decisions in the anti-saccade task was closer to RTs of the correct pro-saccade, with mean RT of 215.61±1.79 ms. A majority of erroneous responses were pro-saccades, so the corresponding distribution mirrored the distribution of correct pro-saccades. Similar results can also be seen in the work of Everling et al. (1998). In this work, however, erroneous pro-saccade had shorter RTs than correct pro-saccade, which was opposite that of the results in Fig. 4B. The average RT for erroneous pro-saccade was 236.68±31.80 ms. The relative large standard error might account for this contradiction. The number of error pro-saccades was not large enough to reflect the whole RT distribution, which

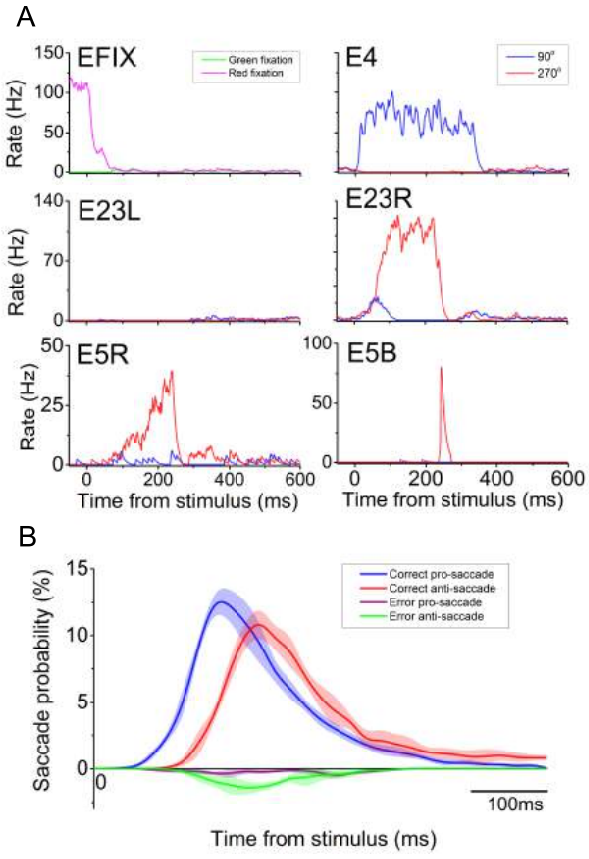

Figure 4. (A) The neural activities of the trained-model in the anti-saccade task. Responses of 90° and 270° preferred population in different layers are shown. (B) Reaction time distribution of pro-saccade and anti-saccade for correct trials and erroneous trials.

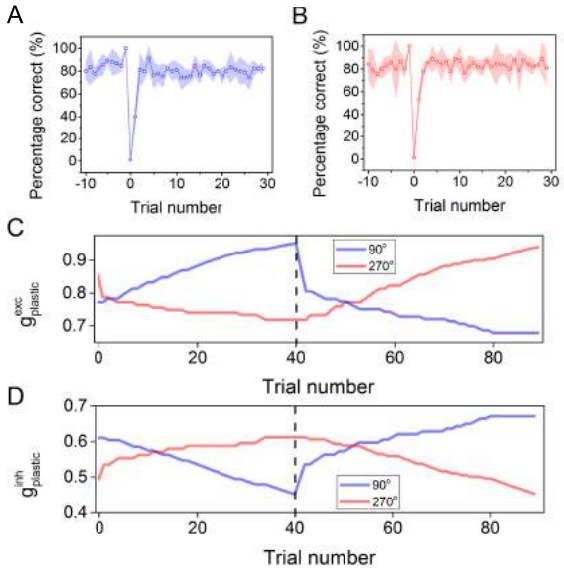

Figure 5. The performance in task switch test between pro-saccade and anti-saccade. (A) and (B) are the changes of correct trial percentage from anti-saccade to pro-saccade and from pro-saccade to anti-saccade, respectively. (C) and (D) are the variations of the excitatory- and inhibitory-based plastic synapse weight in two blocks. These synapses connect the 90° preferred population in E4 to the same side (blue) and the mirror side (red) in E23 or I23. The Dashed line denotes the onset of task switch.

produced a large standard error.

We further performed task switching between pro- and anti-saccade tasks without an explicit instruction. First, we needed to define a new reward rule for trials that occurred just after task switch but have not received the first reward in a block. Here, we let the learning rate, $q = 0.08$ in both the excitatory- and inhibitory-based plastic synapses for these trials. This relatively high learning rate caused the erroneous behavior to be rapidly inhibited until the network knew which choice would be rewarded. The other reward rules followed the training of the anti-saccade task. Fig. 5 illustrates the average performance over successive trials, before and after the task switch. It should be noted that the last trial before the switch was always 100% correct, as the protocol required that the task only switched once 30 correct trials were performed in a block. Trial zero was the first trial after the task switch. In both tasks, the percentage of correct trials abruptly dropped to 0% because the saccade target in the previous block was still considered to be correct. Their performance then increased to approximately 40% in the pro-saccade task and approximately 50% in the anti-saccade task [Fig. 2 in Everling and DeSouza (2005); Fig. 1 in Johnston et al. (2007)]. This was caused by the rapid increase of the inhibitory effect and the dramatic decrease in the excitatory effect to the now incorrect target (Fig. 5C and Fig. 5D). Within 4-5 trials, the proportion of correct trials reached approximately 80% and then stayed at this level, indicating that the model has relearned the tasks in both switching tasks.

3.3. *No-go task*

The network performance in the training process of a no-go task is shown in Fig. 6. A sliding bin with a width of 30 trials and shifted by 1 trial was used to analyze the variation of SPP. A strong firing rate in the 90° preferred population was observed to be mainly concentrated on the early bins (Fig. 6A). As the number of trials increased, the average activities were gradually inhibited. Such inhibition was also demonstrated by the decline of SPP. At the beginning of the task, the SPP of 90° preferred population was distributed at approximately 90%. When training was around the last bin, inhibition dominated the network behavior, inducing the corresponding SPP to be close to 0%. Based on the modulation ratios, the formation of inhibitory dominance depended on the potentiation of the plastic synapses onto the inhibitory neurons (Fig. 6B).

Next, we compared the activities in the go (pro-saccade) trial, correct no-go trial and erroneous no-go trial, and tried to explain how the stop signal canceled a reflexive saccade (Fig. 7). In these trials, the fixation inputs with no color information acted as the stop signals, and the visual stimulus would disappear once the network produced a saccadic signal in E5B. During fixation period, tonic activities could be observed in fixation neurons. However, they gradually ramped down after the onset of the visual signal. Before stop signal onset, the on-going visual signal induced the pro-saccade-related attention for the

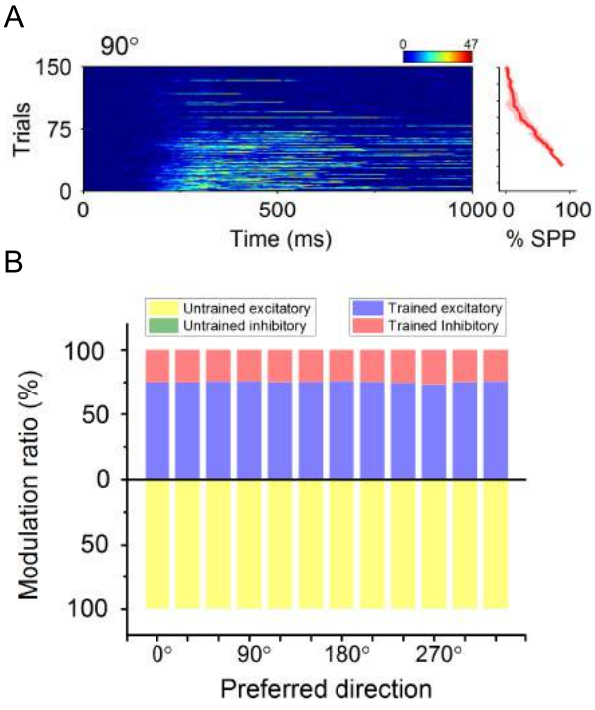

Figure 6. (A) The population firing rate in E5R (left) and saccade percent probability (right) of 90° direction-preferred retinotopic positions in the no-go task. Colors indicate the population firing rate of E5R. (B) Comparison of the modulation ratios of the trained model (red and blue) and untrained model (orange and green). Here these two plastic synapses are between L4 and L23R, which are relevant to the no-go task.

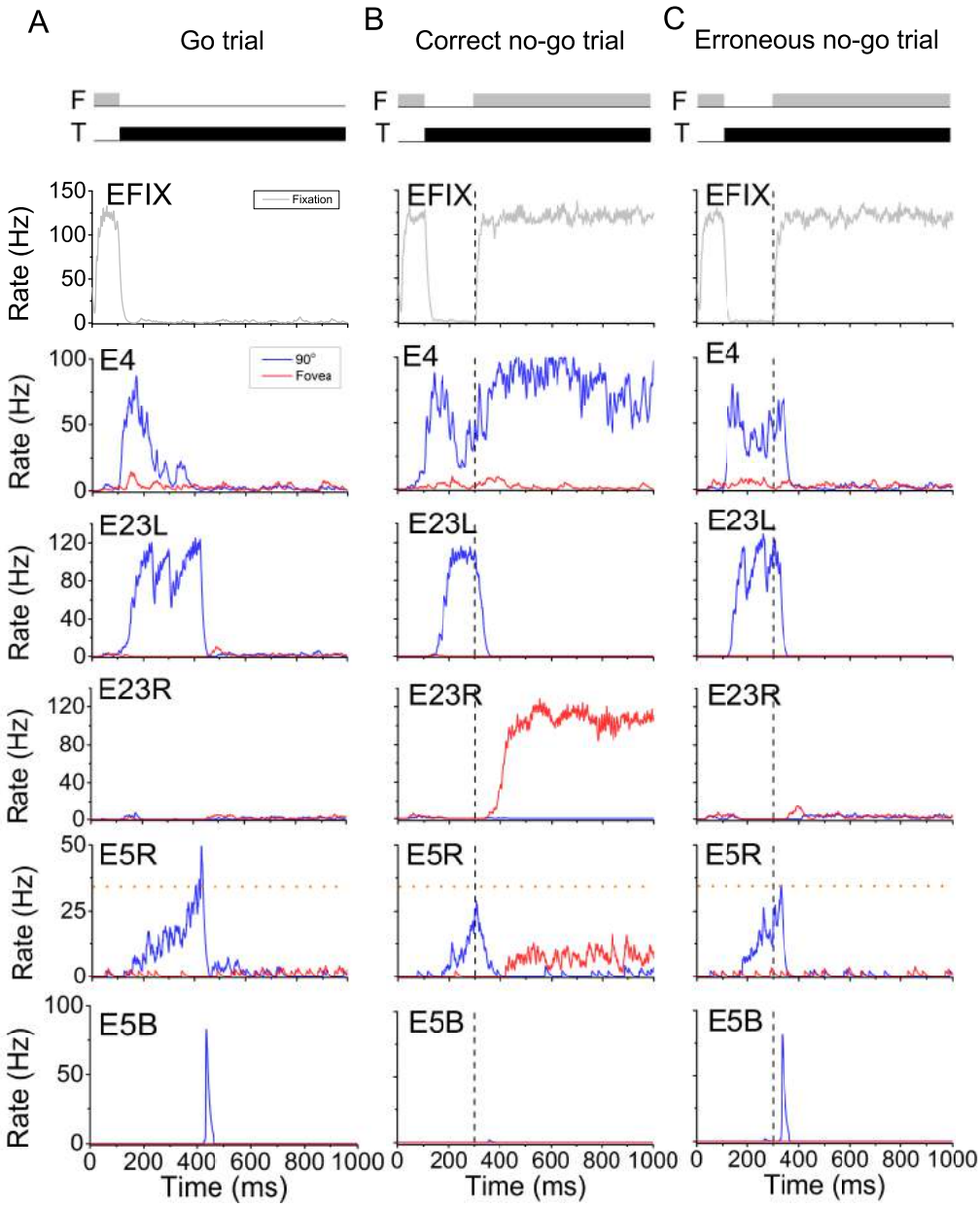

Figure 7. The comparison of the performance of the trained model in three trials: the go trial (A), correct no-go trial (B) and erroneous no-go trial (C). The black dashed line represents the onset time of the stop signal. The orange dotted line is the threshold of E5R. Once the activity of E5R exceed this threshold, E5B will produce a burst that represents a saccade signal. In each chart, the upper panel shows the protocol of the task. The letter F and T represent the fixation input and the visual input, respectively. Colors denote the presence of corresponding inputs.

90° target in E23L. The absence of the stop signal made neurons in E5R persistently transform the attention signal into the motor signal until their activities reached the threshold and resulted in a reflexive saccade in the go trial. In the no-go trial, however, the stop signal, which was presented at 300 ms canceled these pro-saccade-relevant responses before they crossed the threshold. Then, the network began to exhibit no-go-related activities. It could be observed that the fovea population won the subsequent competition at about 400 ms so that the network maintained its attention on the fovea (Fig. 7B). In addition, the erroneous no-go trial occurred because the responses of E5R ramped up to the threshold before the fixation neurons completely activated and inhibited the activities of E23L. The activities of FIX and E5R neurons in these three trials were similar to experimental responses of fixation and movement neurons in the FEF of behaving primates [Hanes et al. (1998), their Fig. 5 and Fig. 7; Schall et al. (2002), their Fig. 5; Brown et al. (2008), their Fig. 5].

The performance of the no-go task can be quantitatively measured by the stop-signal reaction time (SSRT). SSRT is the time difference between the finish time of the stop process and time at which the stop signal is absent (stop-signal delay or SSD); it provides an estimate of the time needed to cancel the saccade movements. However, since it is difficult to measure the

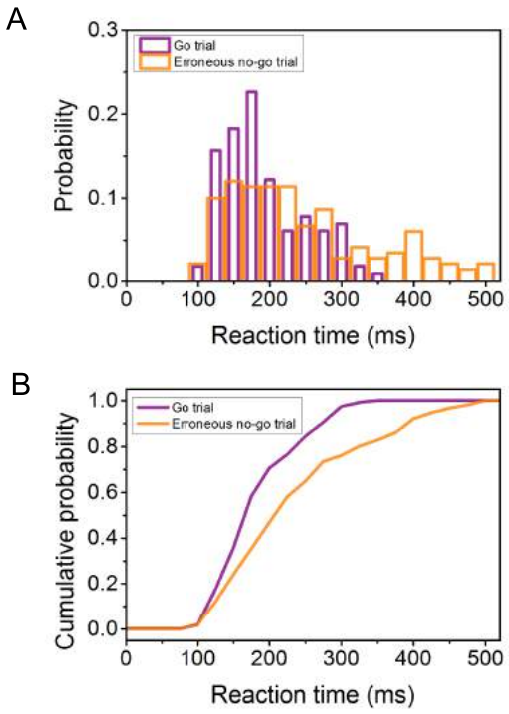

Figure 8. (A) The reaction time distributions of the go trials (purple) and erroneous no-go trials (orange). (B) The cumulative probability functions for reaction times during go trial (purple) and erroneous no-go trial (orange).

canceled time of a correct no-go trial directly, we need to combine the reaction time of the go trial and erroneous no-go trial (RT_{go} and RT_{nogo}) to estimate it (Logan et al., 1984). Continuous trials are performed for the go trial and no-go trial until 100 correct go trials and 100 erroneous no-go trials are obtained. Fig. 8A and Fig. 8B show the distribution and the cumulative probability of the reaction time for these trials, respectively. It can be observed that the distribution probability of RT_{nogo} progressively becomes smaller than that of RT_{go} after 200 ms. After 360 ms, the erroneous no-go trial disappears completely, while a number of go trials still exist in these reaction time intervals, indicating that the go responses are inhibited. This inhibitory control is also emphasized by the gap between the two curves in Fig. 8B. Because the erroneous no-go trials with large reaction time have been inhibited, the corresponding cumulative probability increases at a faster speed [Fig. 2 in Boucher et al. (2007); Fig. 3 in Middlebrooks and Schall (2014); Fig. 2 in Thakkar et al. (2015)]. Note that as the RT_{nogo} of about 97% erroneous no-go trial distributes before 300 ms, we consider it the finish time of the stop process. By subtracting SSD=200 ms, the SSRT of the trained model was 100 ms, while it was around 76 – 96 ms in the experiment reported by Boucher et al. (2007).

3.4. Associative task

The associative task required the network to associate targets based on context. Our model successfully learned the correct cue-saccade association after training. Fig. 9 illustrates two sample trials, one for non-reversal trial (category 1) and the other for reversal trial (category 2) in the trained network. Both of the responses in E4 showed target selectivity and induced task-related attention after the cue stimulus onset. This attention signal was maintained until the saccade was produced [Fig. 3 in Asaad et al. (2000)]. However, it is worth noting that the ongoing attention signal could not make the ramping activity in E5R cross the threshold. This was because the offset of the visual target weakened the attention signal, although it could still maintain firing. Without relatively strong attention activity, the inhibitory role of fixation input on E5R was strengthened, so E5R's activity ramped down [Fig. 3 in Asaad et al. (1998), Fig. 4 in Asaad et al. (2000), Fig. 3 in Histed et al. (2009), Fig. 3 in Puig and Miller (2014)]. When the targets reappeared, the activity of E5R was increased, which could induce a saccade.

Fig. 10A-D illustrates the modulation ratios for four plastic connections. The modulation ratios showed a clear remapping, while the network could only make a reflexive saccade before training. Taking directions in category 1 as examples, they were remapped to the leftward response. The connections from category 1 to 180° in E4→E23L exhibited higher modulation ratios. Note that the modulation ratios of remapping connections were also higher than that of the pro-saccade connections (minor diagonal in Fig. 10A), indicating that the remap-

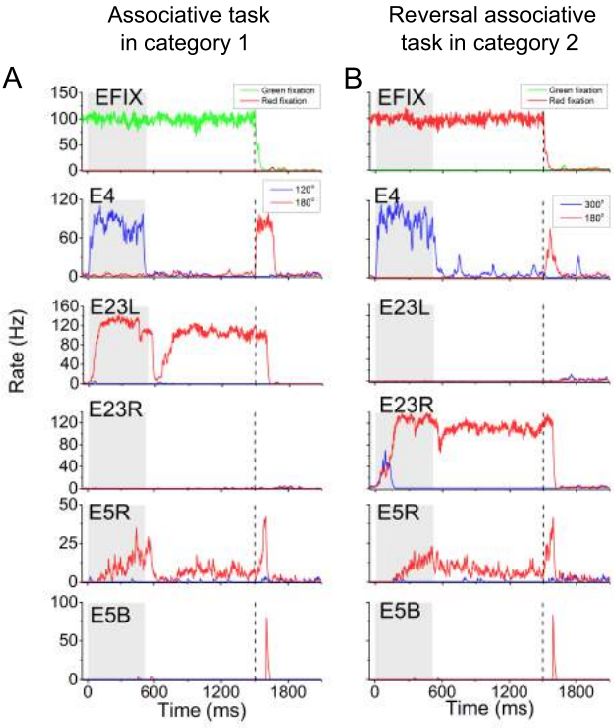

Figure 9. Sample time course of the trained model in the associative task. (A) and (B) are the population firing rate of different layers in the associative task for target (120°) from category 1 and reversal associative task for target (300°) from category 2. The gray area represents the cue period. The black dashed line denotes the onset of visual targets.

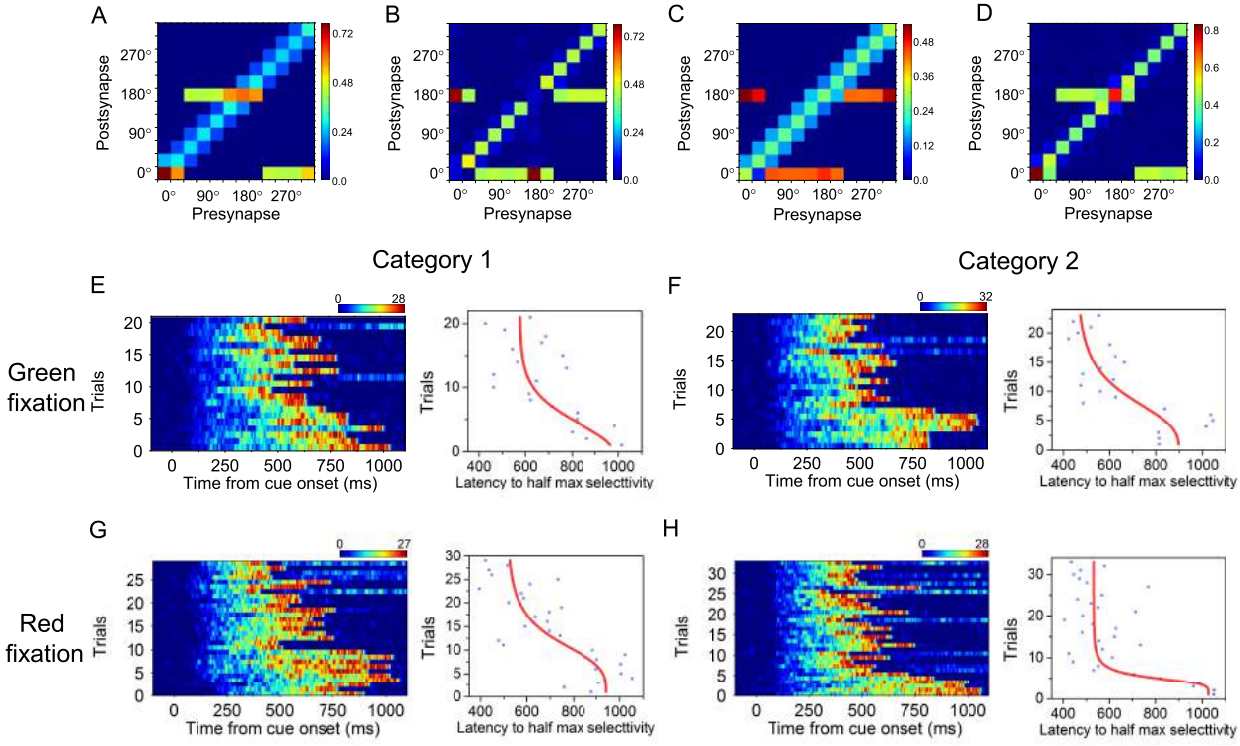

Figure 10. Model behavior in the associative task. (A, B) Modulation ratios under the green fixation for connections E4→E23L (A) and E4→I23L (B). (C, D) Modulation ratios under the red fixation for connections E4→E23R (C) and E4→I23R (D). (E-H) In each of the 8 panels, the left panels are the population firing rates of E5R during the correct trial; right panels show change of latency to half-max selectivity (LHMS). The two categories are: (60°, 90°, 120°, 150°, 180°, 210°) for category 1 and (0°, 30°, 240°, 270°, 300°, 330°) for category 2.

ping activity, instead of the reflexive saccade, has become the overwhelming activity. Meanwhile, the model suppressed the wrong choice targets by enhancing the inhibitory based plastic synapses so that the corresponding modulation ratios of category 1 were relatively large (Fig. 10B). However, we found that the modulation ratios for connections that were related to the reversal trials exhibited different remapping. The excitatory-based plastic synapses in connections from E4 to E23R were strengthened by category 1 to rightward target, so that the corresponding modulation ratios showed a higher level (Fig. 10C), while the leftward response was inhibited when stimulus was presented in directions of category 1 (Fig. 10D). Similar effects could also be observed for the directions in category 2, but the corresponding remappings were opposite.

We also estimated target selectivity, which was defined as the time when half of the maximal activity in E5R was reached. The left panels in Fig. 10E-H depict the correct trials in different conditions. It should be noted that these trials do not include any of the trials that made a correct saccade but focused attention on other directions before the targets onset. Target selectivity tended to appear increasingly earlier as trials progressed [Fig. 6 in Asaad et al. (1998), Fig. 3 in Cromer et al. (2011)]. This tendency was quantitatively indicated by the latency to half max selectivity (LHMS) (right panels in Fig. 10A-D). Early trials seemed to have the largest LHMS. The LHMS of $0-5$ trials in four conditions were distributed between 800 ms and 1100 ms. Subsequently, the LHMS progressively decreased, and finally reached a range of 400-600 ms. Similar variation in LHMS can be observed in a number of works [Fig. 6 in Asaad et al. (1998), Fig. 2 in Pasupathy and Miller (2005)]. Both of the caudate nucleus and prefrontal cortex were reported to be involved in the association task (Pasupathy and Miller, 2005). Compared with the caudate nucleus, our results were more comparable to activities in the prefrontal cortex. During the associative task, the prefrontal cortex showed a gradual decrease of LHMS. In the early trials of the task, the LHMS of the prefrontal cortex were around 900-1100 ms. Then it gradually decreased to a range of 350-500 ms.

Task switching by reversing the cue-saccade pairing, was also performed in the trained model. Similar to the task switching between pro- and anti-saccade, we first defined the reward rule for the trials between reversal onset and the first reward trial in a block. Based on the work of Asaad et al. (1998), we know a priori that the speed of re-learning in the associative task is not as fast as switching between pro-saccades and anti-saccades. Thus, the learning rate for those trials was set at $q = 0.04$, while it otherwise followed the normal associative task training protocol. The performance over successive trials is illustrated in Fig. 11. The model in two cue-saccade pairing reversals exhibits similar performance (Fig. 11A and B). Again, the activity immediately decreases to 0% at task reversal; however, subsequent performance ramped up gradually. It took about 11-12 trials to reach 70% correct. Then, the performance progressively improved to about 80% correct. The relatively slow change

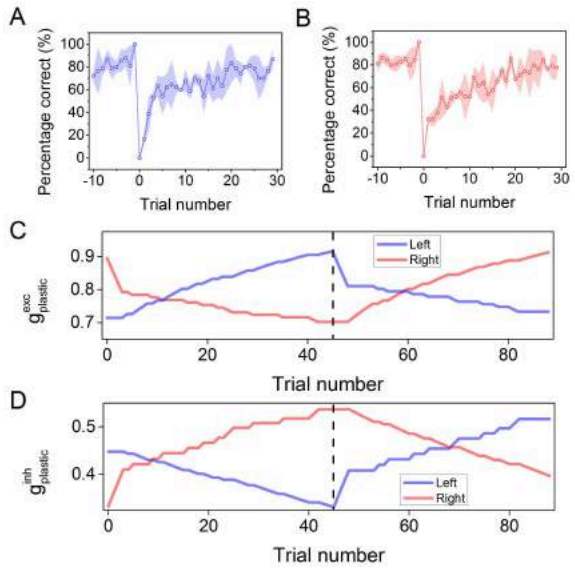

Figure 11. The performance of cue-saccade learning when cue-saccade pairing reverses. (A) and (B) are the changes of correct trial percentage from cue-left trial to cue-right trial and from cue-right learning trial to cue-left trial, respectively. The cue here is 120° preferred stimulus. (C) and (D) are the variations of the excitatory- and inhibitory-based plastic synapse weights in two blocks. These synapses connect the cue to the left (blue) and right (red). The dashed line denotes the onset of reversal.

in excitatory- and inhibitory-based plastic synaptic weights was able to account for the ramping activity (Fig. 11C and D). The model needed about 16 trials after reversal to make the two lines intersect for excitatory-based plastic synapses, while it took 23 trials for inhibitory-based synapses, indicating that the process of suppressing the erroneous choice is relatively slow. Similar ramping activity has been reported in a number of papers (Asaad et al., 1998; Brasted et al., 2005; Pasupathy and Miller, 2005; Histed et al., 2009; Cromer et al., 2011). Their findings are compatible with our simulation results.

4. Discussion

In this study, we presented an extended learning-based microcircuit model of the frontal eye field. This model successfully simulated the cognitive processes of three tasks: the anti-saccade task, no-go task and associative task. These tasks were achieved based on three aspects. First, neurons in the network were assumed to prefer some spatial directions. The neurons that preferred the same direction formed the direction-preferred population. Second, two functional units that were controlled by rule neurons were divided in L23 and allowed the model to show task selectivity. Third, four reward-based plastic synapses projected modulation to the winner-take-all competition in L23, potentiating the correct choices and depressing the erroneous choices. Synaptic modulations were based on the firing rate of the L5B population, which represented the final saccadic decision. Such a learning process may account for the observed animal's adaptive behaviors over multiple task paradigms.

4.1. The mechanism underlying attention and decision-making in choice tasks

Top-down control is typically reported to be a critical mechanism in visual selection (Ardid et al., 2007; Heinen et al., 2014; Lo et al., 2009). In the present model, two plastic modulations from layer 5B, based on a reward-dependent Hebbian learning rule, served as the bias to control saccadic eye movements. These modulations allowed the network to flexibly adjust the neuronal response and adapt to different visual tasks through training over a number of trials, simulating the process of accumulating evidence. In this process, the excitatory and inhibitory modulation acted as two subprocesses: the ability to potentiate a saccade in an instructed direction, and the ability to suppress the reflexive saccade to the visual stimulus (Hutton, 2008; Everling and Fischer, 1998). In the anti-saccade task, erroneous saccades were often attributed to failures of inhibiting wrong choices in neurological studies, which was fully embodied in the early phase of the present training (Crawford et al., 2002; Hutton et al., 1998). Thus, the plastic modulation was more likely to answer the question of how FEF controls the saccadic behaviors based on past experiences and reward expectation.

Layer 2/3, which served as the attention allocator, was endowed with a winner-take-all mechanism. This mechanism limited the network to attend to only one target. However, recent studies imply that it is possible for people to attend to multiple distinct spatial locations simultaneously, but such a split of spatial attention can only be maintained for 100 – 150 ms (Zirnsak et al., 2011; Julien et al., 2012). These reports on attention allocation dynamics may seem to be inconsistent with our simulation results. However, our trained model can show the split of spatial attention (Fig. 4A). Between 0 ms and 110 ms, the responses of two stimulated targets in E23R were activated at the same time, indicating the attention was splitting. After about 110 ms, the pro-saccade won the competition and the network gradually focused its attention on the winner. It seems that these attention splitting activities are not robust, as these activities exhibit in Fig. 9B, but not in Fig. 9A.

4.2. Latency of the anti-saccade

In our trained model, we observed the latency of response time of the anti-saccade, which was consistent with some experimental data. Early studies attributed the latency of the anti-saccade to the application of top-down inhibitory processes. They argued that the inhibitory processes induced anti-saccades to consume more time than pro-saccades so as to shift the response time distribution, making them show a latency (Forbes and Klein, 1996; Machado and Rafal, 2000; Olk and Kingstone, 2003). Recently, this view was extended to the competition resolution mechanism which exerted its role by suppressing an erroneous pre-active pro-saccade and potentiating a correct anti-saccade by attention competition (Engle and Kane, 2004; Kane and Engle, 2003; Unsworth et al., 2011). Our current results imply that the latency shown in the trained model was also triggered by mechanisms in accordance with the competition resolution process. This mechanism was formed by combining the plastic modulations and the winner-take-all mechanism

in layer 2/3. As shown in Fig. 4B, the inhibitory-based plastic modulation depressed the pre-active activities of the reflexive pro-saccade. This modulation made the anti-saccade win the competition of attention and the network reallocated its attention to the anti-saccade.

4.3. The mechanism of task switching

Accumulating evidence has demonstrated that switching between tasks takes time other than instant switching (Chen and Wise, 1995a; Matsumoto et al., 2003; Cromer et al., 2011). A gradual switch pattern of reversal, awaking and relearning has been observed in a number of experimental studies (Everling and DeSouza, 2005; Johnston et al., 2007). Our simulation results also reveal a similar switch pattern. When reversal occurred without an explicit instruction, a monkey still repeated the behavior learned in the preceding block of trials. However, missing rewards for the trials that should be rewarded revealed that the task has been switched, and made the monkey relearn the new task. There are a wide variety of factors that influence the performance of task switching.

Lee et al. (2007) performed a similar experiment and found that systemic blockade of D2R/D3R dopamine receptors, which are related to reward-based learning impaired the reversal learning. Similar effects were seen by overstimulating D2R. In addition, several studies have reported that neural activity conveyed a direction signal progressively earlier during learning with successive trials (Asaad et al., 1998; Pasupathy and Miller, 2005). This evidence emphasizes the role of reward-based learning on switching tasks. The learning rule is also a key component to completion of the tasks in the present study. It assumes that the information of past experiences or reward expectation are stored in the synaptic strength, which can also be altered based on upcoming events. This "synaptic strength" hypothesis is supported by the responses of the frontal lobe and basal ganglia (Jackson et al., 2006). How the synaptic strength changes, and what the corresponding learning rate is within the process of storing information, are still open questions. Besides the relationship between reward and outcome response, the learning rate also depends on the firing rates of the postsynaptic decision neurons, which has been considered in some computational studies (Soltani and Wang, 2006; Barraclough et al., 2004). This effect is the base mechanism for setting different learning rates of excitatory-based and inhibitory-based plastic synapses in the present model.

Task type is another important factor in the performance of task switching. Switching between different tasks shows distinct quantitative effects of reversal learning. The monkey showed fast learning in switching tasks between pro-saccade and anti-saccade: only 3-5 trials were needed after reversal to perform better than 70% correct (Everling and DeSouza, 2005; Johnston et al., 2007). In associative tasks, however, this process did usually take more than 10 trials (Asaad et al., 1998; Pasupathy and Miller, 2005; Histed et al., 2009). Based on these findings, the variance of relearning speed is likely attributed to the task complexity. Our extended model assumed that the learning rate of task switching between pro-saccade and anti-saccade was twice as large as that in associative task. Although the simulation results could match the experimental data, a natural question arose: What is the relationship between task complexity and learning speed. Can it be quantitatively described? These questions need to be resolved by further experiments.

4.4. Comparison with other models

A number of computational models have been proposed to simulate the three choice tasks in this study. For the anti-saccade task and the no-go task, Carpenter (1981) proposed the LATER model that could simulate the neural decision and explain the reaction time distribution. This model assumes that a particular action will be produced when a decision signal increases and reaches the threshold. This mechanism can also be observed in the L5 of our model. When neurons in L5R receive the ongoing attention signals from L23, their activities begin to gradually increase. Once the responses reach the threshold, neurons in L5B immediately make a fast response, indicating a decision has been made. Recently, an increasing number of models are based on the realistic architecture of multiple brain regions, in order to attain a more accurate simulation (Hamker, 2005; Lo et al., 2009; Meeter et al., 2010; Silver et al., 2012). Although some of these models involve FEF dynamics, they place more emphasis on the role of other brain areas such as the basal ganglia and superior colliculus, while keeping the function of the FEF relatively simple (Gancarz and Grossberg, 1999; Mitchell and Zipser, 2003; Cutsuridis et al., 2014). For example, Brown et al. (2004) proposed a functional model connecting the frontal cortex to the basal ganglia circuits, and simulated several oculomotor tasks. This network made a saccade only when cortical inputs indirectly inhibited GABAergic neurons in the substantia Nigra pars reticularis. The FEF block in it just served as a component of planning. In addition, to our knowledge, the number of corresponding models for the associative task is far fewer than that for the anti-saccade task or the no-go task. Fusi et al. (2007) described a learning rule comprising the fast and slow components and used it to simulate a quick forget-and-learn pattern for the conditional associative learning by incorporating a two layer network. They found that the relearning process after task switching is caused by instantly switching between sets of sensorimotor associations. Furthermore, Chersi et al. (2013) developed a cortico-basal ganglia circuit by implementing a delayed associative learning rule that used the reward signal to update the sensorimotor connections at the end of the trial. Besides the learning rule, they also emphasized the role of the prefrontal cortex control. Without the signal from the prefrontal cortex, the model could not adapt to the new cue-response association in the early trials, but had to relearn the task slowly. Compared to the models cited above, our model captures features about the direction preference, learning, attention and motor preparation in the FEF in great detail, although it does not include the other brain areas. The extensions from the original model have highlighted the important aspects of reward-based learning and its role in decision-making.

Acknowledgements

This work was supported by the National Natural Science Foundation of China (Grant No. 11172103 and 11572127).

References

Ardid, S., Wang, X. J., 2013. A tweaking principle for executive control: neuronal circuit mechanism for rule-based task switching and conflict resolution. Journal of Neuroscience 33 (50), 19504–19517.

Ardid, S., Wang, X. J., Compte, A., 2007. An integrated microcircuit model of attentional processing in the neocortex. Journal of Neuroscience 27 (32), 8486–8495.

Asaad, W. F., Rainer, G., Miller, E. K., 1998. Neural activity in the primate prefrontal cortex during associative learning. Neuron 21 (6), 1399–1407.

Asaad, W. F., Rainer, G., Miller, E. K., 2000. Task-specific neural activity in the primate prefrontal cortex. Journal of Neurophysiology 84 (1), 451–459.

Baldassarre, G., Mannella, F., Fiore, V. G., Redgrave, P., Gurney, K., Mirolli, M., 2013. Intrinsically motivated action-outcome learning and goal-based action recall: a system-level bio-constrained computational model. Neural Networks 41, 168–187.

Barraclough, D. J., Conroy, M. L., Lee, D., 2004. Prefrontal cortex and decision making in a mixed-strategy game. Nature neuroscience 7 (4), 404–410.

Bell, A., Everling, S., Munoz, D., 2000. Influence of stimulus eccentricity and direction on characteristics of pro-and antisaccades in non-human primates. Journal of Neurophysiology 84 (5), 2595–2604.

Bichot, N. P., Schall, J. D., Thompson, K. G., 1996. Visual feature selectivity in frontal eye fields induced by experience in mature macaques. Nature 381, 697–699.

Blank, H., Biele, G., Heekeren, H. R., Philiastides, M. G., 2013. Temporal characteristics of the influence of punishment on perceptual decision making in the human brain. Journal of Neuroscience 33 (9), 3939–3952.

Boucher, L., Palmeri, T. J., Logan, G. D., Schall, J. D., 2007. Inhibitory control in mind and brain: an interactive race model of countermanding saccades. Psychological review 114 (2), 376–397.

Brasted, P. J., Bussey, T. J., Murray, E. A., Wise, S. P., 2005. Conditional motor learning in the nonspatial domain: effects of errorless learning and the contribution of the fornix to one-trial learning. Behavioral neuroscience 119 (3), 662–676.

Brown, J. W., Bullock, D., Grossberg, S., 2004. How laminar frontal cortex and basal ganglia circuits interact to control planned and reactive saccades. Neural Networks 17 (4), 471–510.

Brown, J. W., Hanes, D. P., Schall, J. D., Stuphorn, V., 2008. Relation of frontal eye field activity to saccade initiation during a countermanding task. Experimental brain research 190 (2), 135–151.

Bruce, C. J., Goldberg, M. E., 1985. Primate frontal eye fields. i. single neurons discharging before saccades. Journal of Neurophysiology 53 (3), 603–635.

Carpenter, R., 1981. Oculomotor procrastination. Eye movements: Cognition and visual perception, 237–246.

Chaumon, M., Kveraga, K., Barrett, L. F., Bar, M., 2014. Visual predictions in the orbitofrontal cortex rely on associative content. Cerebral Cortex 24 (11), 2899–2907.

Chen, L. L., Wise, S. P., 1995a. Neuronal activity in the supplementary eye field during acquisition of conditional oculomotor associations. Journal of Neurophysiology 73 (3), 1101–1121.

Chen, L. L., Wise, S. P., 1995b. Supplementary eye field contrasted with the frontal eye field during acquisition of conditional oculomotor associations. Journal of Neurophysiology 73 (3), 1122–1134.

Chersi, F., Mirolli, M., Pezzulo, G., Baldassarre, G., 2013. A spiking neuron model of the cortico-basal ganglia circuits for goal-directed and habitual action learning. Neural Networks 41, 212–224.

Connolly, P. M., Bennur, S., Gold, J. I., 2009. Correlates of perceptual learning in an oculomotor decision variable. The Journal of Neuroscience 29 (7), 2136–2150.

Crawford, T. J., Bennett, D., Lekwuwa, G., Shaunak, S., Deakin, J. F. W., 2002. Cognition and the inhibitory control of saccades in schizophrenia and Parkinson's disease. Progress in Brain Research. pp. 449–466.

Cromer, J. A., Machon, M., Miller, E. K., 2011. Rapid association learning in the primate prefrontal cortex in the absence of behavioral reversals. Journal of cognitive neuroscience 23 (7), 1823–1828.

Cutsuridis, V., Kumari, V., Ettinger, U., 2014. Antisaccade performance in schizophrenia: a neural model of decision making in the superior colliculus. Front Neurosci 8, 13–13.

Destexhe, A., Rudolph, M., Fellous, J.-M., Sejnowski, T. J., 2001. Fluctuating synaptic conductances recreate in vivo-like activity in neocortical neurons. Neuroscience 107 (1), 13–24.

Douglas, R. J., Martin, K. A., Whitteridge, D., 1991. An intracellular analysis of the visual responses of neurones in cat visual cortex. The Journal of physiology 440, 659–696.

Drea, C. M., Wallen, K., 1999. Low-status monkeys "play dumb" when learning in mixed social groups. Proceedings of the National Academy of Sciences of the United States of America 96 (22), 12965–12969.

Drugowitsch, J., Moreno-Bote, R., Churchland, A. K., Shadlen, M. N., Pouget, A., 2012. The cost of accumulating evidence in perceptual decision making. Journal of Neuroscience 32 (11), 3612–3628.

Engel, T. A., Wang, X. J., 2011. Same or different? a neural circuit mechanism of similarity-based pattern match decision making. Journal of Neuroscience 31 (19), 6982–6996.

Engle, R. W., Kane, M. J., 2004. Executive attention, working memory capacity, and a two-factor theory of cognitive control. Psychology of Learning and Motivation 44, 145–200.

Everling, S., DeSouza, J. F., 2005. Rule-dependent activity for prosaccades and antisaccades in the primate prefrontal cortex. Journal of Cognitive Neuroscience 17 (9), 1483–1496.

Everling, S., Dorris, M. C., Klein, R. M., Munoz, D. P., 1999. Role of primate superior colliculus in preparation and execution of anti-saccades and pro-saccades. The Journal of Neuroscience 19 (7), 2740–2754.

Everling, S., Dorris, M. C., Munoz, D. P., 1998. Reflex suppression in the anti-saccade task is dependent on prestimulus neural processes. Journal of Neurophysiology 80 (3), 1584–1589.

Everling, S., Fischer, B., 1998. The antisaccade: a review of basic research and clinical studies. Neuropsychologia 36 (9), 885–899.

Everling, S., Munoz, D. P., 2000. Neuronal correlates for preparatory set associated with pro-saccades and anti-saccades in the primate frontal eye field. The Journal of Neuroscience 20 (1), 387–400.

Ferrera, V. P., Cohen, J. K., Lee, B. B., 1999. Activity of prefrontal neurons during location and color delayed matching tasks. Neuroreport 10 (6), 1315–1322.

Forbes, K., Klein, R. M., 1996. The magnitude of the fixation offset effect with endogenously and exogenously controlled saccades. Journal of Cognitive Neuroscience 8 (4), 344–352.

Freedman, D. J., Assad, J. A., 2006. Experience-dependent representation of visual categories in parietal cortex. Nature 443 (7107), 85–88.

Fusi, S., Asaad, W. F., Miller, E. K., Wang, X. J., 2007. A neural circuit model of flexible sensorimotor mapping: learning and forgetting on multiple timescales. Neuron 54 (2), 319–333.
URL http://www.ncbi.nlm.nih.gov/pubmed/17442251

Gancarz, G., Grossberg, S., 1999. A neural model of saccadic eye movement control explains task-specific adaptation. Vision research 39 (18), 3123–3143.

Gold, J. I., Shadlen, M. N., 2002. Banburismus and the brain: decoding the relationship between sensory stimuli, decisions, and reward. Neuron 36 (2), 299–308.

Gold, J. I., Shadlen, M. N., 2003. The influence of behavioral context on the representation of a perceptual decision in developing oculomotor commands. The Journal of Neuroscience 23 (2), 632–651.

Gottlieb, J., Hayhoe, M., Hikosaka, O., Rangel, A., 2014. Attention, reward, and information seeking. Journal of Neuroscience 34 (46), 15497–15504.

Hamker, F. H., 2005. The reentry hypothesis: the putative interaction of the frontal eye field, ventrolateral prefrontal cortex, and areas v4, it for attention and eye movement. Cerebral Cortex 15 (4), 431–447.

Hanes, D. P., Patterson, W. F., Schall, J. D., 1998. Role of frontal eye fields in countermanding saccades: visual, movement, and fixation activity. Journal of Neurophysiology 79 (2), 817–834.

Hansel, D., van Vreeswijk, C., 2012. The mechanism of orientation selectivity in primary visual cortex without a functional map. Journal of Neuroscience 32 (12), 4049–4064.

Hasegawa, R. P., Peterson, B. W., Goldberg, M. E., 2004. Prefrontal neurons coding suppression of specific saccades. Neuron 43 (3), 415–425.

Heinen, K., Feredoes, E., Weiskopf, N., Ruff, C. C., Driver, J., 2014. Direct evidence for attention-dependent influences of the frontal eye-fields on feature-

responsive visual cortex. Cerebral Cortex 24 (11), 2815–2821.
Heinzle, J., Hepp, K., Martin, K. A., 2007. A microcircuit model of the frontal eye fields. Journal of Neuroscience 27 (35), 9341–9353.
Histed, M. H., Pasupathy, A., Miller, E. K., 2009. Learning substrates in the primate prefrontal cortex and striatum: sustained activity related to successful actions. Neuron 63 (2), 244–253.
Hoshi, E., Shima, K., Tanji, J., 1998. Task-dependent selectivity of movement-related neuronal activity in the primate prefrontal cortex. Journal of Neurophysiology 80 (6), 3392–3397.
Hubel, D. H., Wiesel, T. N., 1959. Receptive fields of single neurones in the cat's striate cortex. The Journal of Physiology 148, 574–591.
Hutton, S., Crawford, T. J., Puri, B., Duncan, L.-J., Chapman, M., Kennard, C., Barnes, T., Joyce, E., 1998. Smooth pursuit and saccadic abnormalities in first-episode schizophrenia. Psychological Medicine 28 (03), 685–692.
Hutton, S. B., 2008. Cognitive control of saccadic eye movements. Brain and Cognition 68 (3), 327–340.
Jackson, A., Mavoori, J., Fetz, E. E., 2006. Long-term motor cortex plasticity induced by an electronic neural implant. Nature 444 (7115), 56–60.
Johnston, K., DeSouza, J. F., Everling, S., 2009. Monkey prefrontal cortical pyramidal and putative interneurons exhibit differential patterns of activity between prosaccade and antisaccade tasks. The Journal of Neuroscience 29 (17), 5516–5524.
Johnston, K., Everling, S., 2006. Neural activity in monkey prefrontal cortex is modulated by task context and behavioral instruction during delayed-match-to-sample and conditional prosaccadełantisaccade tasks. Journal of Cognitive Neuroscience 18 (5), 749–765.
Johnston, K., Levin, H. M., Koval, M. J., Everling, S., 2007. Top-down control-signal dynamics in anterior cingulate and prefrontal cortex neurons following task switching. Neuron 53 (3), 453–462.
Julien, D., Hamker, F. H., Rufin, V. R., 2012. Attentional selection of noncontiguous locations: the spotlight is only transiently "split". Social Science Electronic Publishing 12 (120), 409–425.
Kan, J. Y., Niel, U., Dorris, M. C., 2012. Evidence for a link between the experiential allocation of saccade preparation and visuospatial attention. Journal of Neurophysiology 107 (5), 1413–1420.
Kane, M. J., Engle, R. W., 2003. Working-memory capacity and the control of attention: the contributions of goal neglect, response competition, and task set to stroop interference. Journal of Experimental Psychology: General 132 (1), 47–70.
Law, C.-T., Gold, J. I., 2009. Reinforcement learning can account for associative and perceptual learning on a visual-decision task. Nature Neuroscience 12 (5), 655–663.
Leathers, M. L., Olson, C. R., 2012. In monkeys making value-based decisions, lip neurons encode cue salience and not action value. Science 338 (6103), 132–135.
Lee, B., Groman, S., London, E. D., Jentsch, J. D., 2007. Dopamine d2/d3 receptors play a specific role in the reversal of a learned visual discrimination in monkeys. Neuropsychopharmacology 32 (10), 2125–2134.
Lee, K. M., Keller, E. L., 2008. Neural activity in the frontal eye fields modulated by the number of alternatives in target choice. Journal of Neuroscience 28 (9), 2242–2251.
Lewis, C. M., Baldassarre, A., Committeri, G., Romani, G. L., Corbetta, M., 2009. Learning sculpts the spontaneous activity of the resting human brain. Proceedings of the National Academy of Sciences 106 (41), 17558–17563.
Li, C. Y., Creutzfeldt, O., 1984. The representation of contrast and other stimulus parameters by single neurons in area 17 of the cat. Pflugers Archiv : European Journal of Physiology 401 (3), 304–314.
Lo, C. C., Boucher, L., Pare, M., Schall, J. D., Wang, X. J., 2009. Proactive inhibitory control and attractor dynamics in countermanding action: a spiking neural circuit model. Journal of Neuroscience 29 (28), 9059–9071.
Logan, G. D., Cowan, W. B., Davis, K. A., 1984. On the ability to inhibit simple and choice reaction time responses: a model and a method. Journal of Experimental Psychology: Human Perception and Performance 10 (2), 276–291.
Luhmann, C. C., Chun, M. M., Yi, D.-J., Lee, D., Wang, X.-J., 2008. Neural dissociation of delay and uncertainty in intertemporal choice. Journal of Neuroscience 28 (53), 14459–14466.
Machado, L., Rafal, R., 2000. Control of eye movement reflexes. Experimental Brain Research 135 (1), 73–80.
Matsumoto, K., Suzuki, W., Tanaka, K., 2003. Neuronal correlates of goal-based motor selection in the prefrontal cortex. Science 301 (5630), 229–232.
Meeter, M., Van der Stigchel, S., Theeuwes, J., 2010. A competitive integration model of exogenous and endogenous eye movements. Biological cybernetics 102 (4), 271–291.
Middlebrooks, P. G., Schall, J. D., 2014. Response inhibition during perceptual decision making in humans and macaques. Attention, Perception, & Psychophysics 76 (2), 353–366.
Mitchell, J. F., Zipser, D., 2003. Sequential memory-guided saccades and target selection: a neural model of the frontal eye fields. Vision Research 43 (25), 2669–2695.
Moreno-Bote, R., Parga, N., 2004. Role of synaptic filtering on the firing response of simple model neurons. Physical Review Letters 92 (2), 537–547.
Moreno-Bote, R., Parga, N., 2010. Response of integrate-and-fire neurons to noisy inputs filtered by synapses with arbitrary timescales: Firing rate and correlations. Neural computation 22 (6), 1528–1572.
Munoz, D. P., Everling, S., 2004. Look away: the anti-saccade task and the voluntary control of eye movement. Nature Reviews Neuroscience 5 (3), 218–228.
Noorani, I., 2014. Later models of neural decision behavior in choice tasks. Frontiers in Integrative Neuroscience 8, 67.
Nowak, L. G., Sanchez-Vives, M. V., McCormick, D. A., 2008. Lack of orientation and direction selectivity in a subgroup of fast-spiking inhibitory interneurons: cellular and synaptic mechanisms and comparison with other electrophysiological cell types. Cerebral Cortex 18 (5), 1058–1078.
Olk, B., Kingstone, A., 2003. Why are antisaccades slower than prosaccades? a novel finding using a new paradigm. Neuroreport 14 (1), 151–155.
Pasupathy, A., Miller, E. K., 2005. Different time courses of learning-related activity in the prefrontal cortex and striatum. Nature 433 (7028), 873–876.
Pfeiffer, M., Nessler, B., Douglas, R. J., Maass, W., 2010. Reward-modulated hebbian learning of decision making. Neural Computation 22 (6), 1399–1444.
Platt, M. L., Glimcher, P. W., 1999. Neural correlates of decision variables in parietal cortex. Nature 400 (6741), 233–238.
Pleger, B., Ruff, C. C., Blankenburg, F., Bestmann, S., Wiech, K., Stephan, K. E., Capilla, A., Friston, K. J., Dolan, R. J., 2006. Neural coding of tactile decisions in the human prefrontal cortex. Journal of Neuroscience 26 (48), 12596–12601.
Puig, M. V., Miller, E. K., 2014. Neural substrates of dopamine d2 receptor modulated executive functions in the monkey prefrontal cortex. Cerebral Cortex 25 (9), 2980–2987.
Ringach, D. L., Shapley, R. M., Hawken, M. J., 2002. Orientation selectivity in macaque v1: Diversity and laminar dependence. Journal of Neuroscience 22 (13), 5639–5651.
Salinas, E., 2003. Background synaptic activity as a switch between dynamical states in a network. Neural Computation 15 (7), 1439–1475.
Salinas, E., 2004. Context-dependent selection of visuomotor maps. BMC Neuroscience 5, 116–119.
Sander, V., Soper, B., Everling, S., 2010. Nonhuman primate event-related potentials associated with pro-and anti-saccades. NeuroImage 49 (2), 1650–1658.
Savine, A. C., Braver, T. S., 2010. Motivated cognitive control: reward incentives modulate preparatory neural activity during task-switching. Journal of Neuroscience 30 (31), 10294–10305.
Schall, J. D., Hanes, D. P., Taylor, T. L., 2000. Neural control of behavior: countermanding eye movements. Psychological Research 63 (3-4), 299–307.
Schall, J. D., Stuphorn, V., Brown, J. W., 2002. Monitoring and control of action by the frontal lobes. Neuron 36 (2), 309–322.
Schiller, P. H., Finlay, B. L., Volman, S. F., 1976. Quantitative studies of single-cell properties in monkey striate cortex. i. spatiotemporal organization of receptive fields. Journal of Neurophysiology 39 (6), 1288–1319.
SchlagRey, M., Amador, N., Sanchez, H., Schlag, J., 1997. Antisaccade performance predicted by neuronal activity in the supplementary eye field. Nature 390 (6658), 398–401.
Shushruth, S., Mangapathy, P., Ichida, J. M., Bressloff, P. C., Schwabe, L., Angelucci, A., 2012. Strong recurrent networks compute the orientation tuning of surround modulation in the primate primary visual cortex. Journal of Neuroscience 32 (1), 308–321.
Silver, M. R., Grossberg, S., Bullock, D., Histed, M. H., Miller, E. K., 2012. A neural model of sequential movement planning and control of eye movements: Item-order-rank working memory and saccade selection by the supplementary eye fields. Neural Networks 26, 29–58.
Soltani, A., Wang, X. J., 2006. A biophysically based neural model of matching

law behavior: melioration by stochastic synapses. Journal of Neuroscience 26 (14), 3731–3744.

Thakkar, K. N., Schall, J. D., Logan, G. D., Park, S., 2015. Cognitive control of gaze in bipolar disorder and schizophrenia. Psychiatry research 225 (3), 254–262.

Tseng, P., Chang, C. F., Chiau, H. Y., Liang, W. K., Liu, C. L., Hsu, T. Y., Hung, D. L., Tzeng, O. J., Juan, C. H., 2013. The dorsal attentional system in oculomotor learning of predictive information. Frontiers in Human Neuroscience 7, 404–404.

Unsworth, N., Spillers, G. J., Brewer, G. A., McMillan, B., 2011. Attention control and the antisaccade task: a response time distribution analysis. Acta Psychologica 137 (1), 90–100.

White, I. M., Wise, S. P., 1999. Rule-dependent neuronal activity in the prefrontal cortex. Experimental brain research 126 (3), 315–335.

Wu, Z., Guo, A., 2011. A model study on the circuit mechanism underlying decision-making in drosophila. Neural Networks 24 (4), 333–344.

Zirnsak, M., Beuth, F., Hamker, F. H., 2011. Split of spatial attention as predicted by a systems-level model of visual attention. European Journal of Neuroscience 33 (11), 2035–2045.